

Room-Temperature Dual Excitonic Emission from Amorphous ZnO

This article has been downloaded from IOPscience. Please scroll down to see the full text article.

2003 Chinese Phys. Lett. 20 696

(<http://iopscience.iop.org/0256-307X/20/5/330>)

View [the table of contents for this issue](#), or go to the [journal homepage](#) for more

Download details:

IP Address: 159.226.165.151

The article was downloaded on 05/09/2012 at 05:10

Please note that [terms and conditions apply](#).

Room-Temperature Dual Excitonic Emission from Amorphous ZnO *

WANG Zhi-Jian(王之建)¹, WANG Zhi-Jun(王志军)¹, ZHANG Li-Gong(张立功)¹,
YUAN Jin-Shan(元金山)¹, YAN Sheng-Gang(阎圣刚)², WANG Chun-Yan(王春燕)²

¹Laboratory of Excited State Processes, Changchun Institute of Optics, Fine Mechanics and Physics,
Chinese Academy of Sciences, Changchun 130021

²School of Chemical Engineering, Dalian University of Technology, Dalian 116012

(Received 10 December 2002)

Optical properties of amorphous ZnO have been investigated at room temperature. It is demonstrated that the ultraviolet emission components due to the recombination of two different excitons were verified by examining their relative energy positions and ultraviolet integrated photoluminescence intensity dependence on reaction time. The dual excitonic emissions are derived from amorphous ZnO and crystallized ZnO nanocrystallite, respectively. On the optimized condition, the photoluminescence spectrum of amorphous ZnO shows a strong ultraviolet emission while the visible emission is almost fully quenched. The enhanced ultraviolet emission is attributed to quantum confinement effect.

PACS: 61.43.Er, 61.46.+w, 78.55.Et, 78.55.-m

As a wide band gap semiconductor, ZnO has attracted much attention due to the strong commercial desire for blue and ultraviolet light emitters and detectors.^[1-6] Low threshold for optical pumping and larger exciton binding energy (about 60 meV), which in principle, should allow for efficient excitonic lasing mechanisms operated at room or even higher temperatures.^[7]

In recent years, intensive development of nanomaterials and creating new technologies such as quantum well lasers has constituted an important branch of optical materials.^[8,9] Because of the structural and electronic confinement effects of these materials, studies on both size and shape dependences of their physical properties as well as on the fabrication of potential devices are of particular interest and importance.^[10] In the past decade, various methods have been employed to study nano-sized ZnO material.^[11,12] In most of the previous work, visible emission dominates the Photoluminescence (PL) spectra of ZnO, while ultraviolet (UV) emission is often weaker than that of visible emission.^[13,14] There is little work reported on luminescence of amorphous ZnO with strong UV emission, while the visible emission was fully quenched. In this Letter, we report, for the first time to our best knowledge, the observation of strong UV emission from amorphous ZnO while the visible emission is almost fully quenched at room temperature. The UV spectra are consisted of two emission peaks. Study on PL spectra of different reaction time suggested that dually excitonic emissions are originated from amorphous ZnO and nanocrystalline ZnO, respectively. Amorphous materials are composed of localized states and expanded state. In our experiment, the complex water removed the band tail and swept the band gap de-

fect, so it displays characteristics of analogously crystal ZnO.^[15] The amorphous ZnO capped or modified the nanocrystalline ZnO, where the structure displays quantum-dot properties, which greatly decreases the surface trapping and non-radiative charge carrier recombination process with the particles. The strongly enhanced optical emission is associated with quantum confinement effect.

The typical preparation of amorphous ZnO is described as follows. We mix 2.2 g (10 mmol) Zn(CH₃COO)₂·2H₂O and 2 g (23.8 mmol) NaHCO₃ at room temperature. The mixture was pyrolyzed at 160°C for 3 h. Zn(CH₃COO)₂ is changed into amorphous ZnO while the NaHCO₃ is turned into the corresponding CH₃COONa and eventually is washed away by deionized water. Consequently, a white, highly fluffy, voluminous floccular mass in appearance amorphous ZnO powder can be obtained through the thermal decomposition process. The microstructure of the amorphous ZnO was observed by JEOL-2010 transmission-electron microscopy (TEM). The structure of the amorphous ZnO was analysed by Rigaku RU-200B rotax x-ray diffractometer with Cu K_α radiation ($\lambda = 1.5406 \text{ \AA}$). In low-dimensional materials, effects of their geometrical restrictions are well reflected in their optical responses. In turn, the photoluminescence is good measures to explore the intrinsic nature of low-dimensional systems. The PL spectra were measured with a Hitachi MPF-4 fluorescence spectrophotometer by using a 150 W xenon lamp with an excitation wavelength of 325 nm at room temperature.

In the thermal decomposition process, the by-product plays an important role to control the particle growth and agglomeration. The method pro-

posed here is focused on a strategy for separating these amorphous ZnO by the by-product CH_3COONa that can distribute on the formed ZnO surface to prevent them from the agglomeration. Moreover, such a compound can be converted into amorphous ZnO by dissolution of CH_3COONa . In the experiment, when the mixture is allowed to decompose at certain temperature, the amorphous ZnO was formed quickly and was slowly changed into crystal ZnO at the same time. The growth rate strongly depends on decomposition temperature.

Figure 1 shows a typical amorphous ZnO TEM image. The TEM image shows that amorphous ZnO distributes disorderly and has no distinct morphology, which show a high fluffy, voluminous floccular mass and high disorder in appearance. When we try to obtain a selected area electron diffraction (SEAD) patterns, the patterns cannot be obtained. It is clear that sample does not have obvious crystal structures. Experimental x-ray diffraction is used to detect the amorphous ZnO. Figure 2(a) barely shows any obvious diffraction peaks, only some very weak, small peaks which come from crystallized ZnO. Thermal gravity analysis explains that 3–5% of amorphous ZnO product has been turned into nanocrystalline ZnO.



Fig. 1. Typical TEM image of amorphous ZnO.

Figure 3 gives the PL spectra of amorphous ZnO at room temperature. The amorphous ZnO shows an extremely enhanced UV emission of about 300% over that of the high quality crystal ZnO (about 10 nm diameter, visible emission fully quenched),^[16] while the visible emission is very weak. Spectrum separation of the UV components shows that the UV spectrum of amorphous ZnO consists of two emitting bands, including a strong UV emission at around 378 nm, a weak UV band at 355 nm. As is well known, bound excitons which are related to Li^+ or Na^+ centres in

crystalline ZnO have been reported by several groups

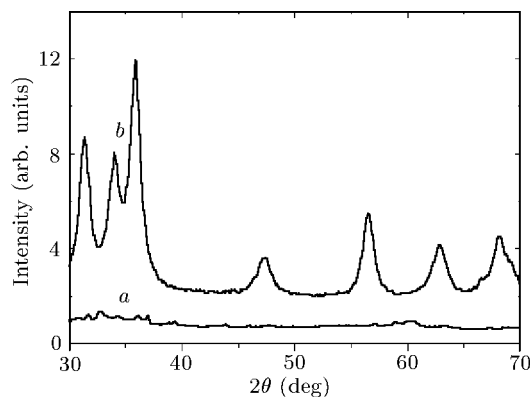


Fig. 2. Typical XRD data corresponding to (a) amorphous ZnO and (b) crystalline ZnO.

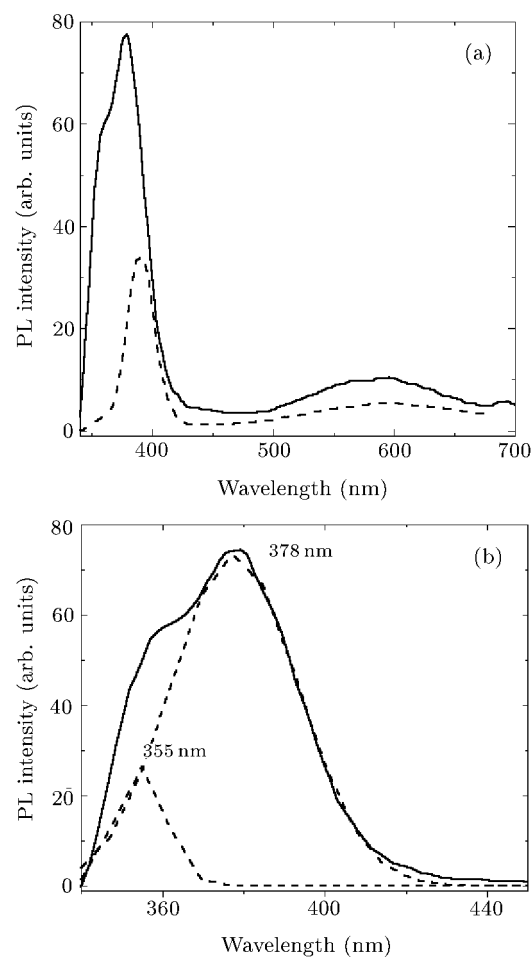


Fig. 3. (a) Room-temperature PL spectra of amorphous ZnO (solid line) and reference nanocrystalline ZnO (dashed line). The sample is taken at 160°C for 3 h. (b) Spectra separation procedure of the excitonic components.

before.^[17–19] Na^+ is an inevitable dopant in our samples since we used NaHCO_3 for synthesis precursor, so the UV peaks are associated with bound excitonic emission. The two excitonic emissions play an impor-

tant role in increasing ultraviolet integrated intensity. To provide more information for understanding the origin of the UV-emission, we have studied the optical properties of amorphous ZnO ageing with different heat treatment times.

Figure 4 shows the PL emission spectra of samples ageing at 160°C for different times. First, the PL emission band shifts to lower energies upon prolonging the heat treatment. Second, the PL spectrum exhibits two kinds of UV-excitonic emission. This feature becomes less pronounced when the amorphous ZnO is fully crystallized. Third, the PL spectra show strong UV-emission while the visible band (about 590 nm) is relatively weak. Nevertheless, the detailed visible emission required further studies and goes beyond the scope of this paper. In sample *a*, it seems that there is only a strong UV-emission, but spectrum separation shows that it is also composed of two excitonic emissions, which correspond to the peaks at 355 nm and 374 nm, respectively. Upon increasing the heat treatment, two peaks are obviously appeared on the UV spectra. We believed that the main peak is dominated by radiative recombination of nanocrystalline ZnO, denoted by *B*. A shoulder denoted by *L* appears on the high-energy side of the *B* band. The *L* emission band is localized at 355 nm. The lowest trace shows the PL spectrum taken from a sample thermal decomposition for 72 h, where only a commonly excitonic emission located at 388 nm for nanocrystalline ZnO. For clarity, the heat treatment time dependence of the peak energy and UV integrated intensity of these two bands are shown in Figs. 5(a) and 5(b), respectively.

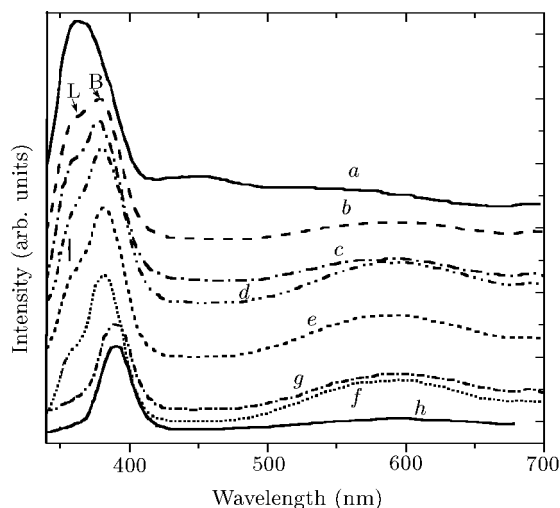


Fig. 4. Room-temperature PL spectra of samples grown at 160°C for different heat treatment times: (a) 0.5 h, (b) 1 h, (c) 1.5 h, (d) 2 h, (e) 3 h, (f) 5 h, (g) 16 h, and (h) 72 h.

Traditionally, the PL spectrum of amorphous material often appears in a long wave region, because there is a band tail in the band gap, which always

causes redshift of the PL spectrum. In our previous work,^[15] there is a molecular water complex with amorphous ZnO, where the complex water sweeps the dangling band and the surface band, so removes the band tail and explains the characteristics of expanded states, something like that of ZnO nanocrystallite. As can be seen in Fig. 5(a), the peak energy of the *L* band appears greatly shift to higher energies 355 nm and barely change with the increasing reaction time upon heat treatment up to fully crystallite. The *B* band peak energy is lower than that of the *L* band and slowly decreases from 374 nm to 388 nm with prolonging the heat treatment time. According to the previous reports,^[13,20] the particle-size dependence of band enlargement can be used to calculate the diameter of nanocrystalline ZnO, where $E_g = 3.22$ eV, $m_e^* = 0.24$, $m_h^* = 0.45$ and $\epsilon = 3.7$. The radius of nanocrystalline ZnO is about 1–1.5 nm when the heat treatment time is controlled under 0.5–4 h, where the size is smaller than that of exciton Bohr radius (~ 1.8 nm),^[21] showing an obvious blueshift to high energy. The reaction time dependence of the integrated UV emission intensity of the *L* and *B* bands is shown in Fig. 5(b). The *L* curve decreases gradually and disappears lastly but the *B* curve appears from lower to the maximum intensity rapidly and then decreases slowly. At the early stage of heat treatment, the precursor quickly changes into amorphous ZnO, however, the nanocrystalline just begins to form at that time, so the integrated *B* intensity is weak. When the precursor was fully changed into amorphous ZnO and nanocrystalline ZnO was just nucleated, The quantum-dot structure of amorphous ZnO/nanocrystalline ZnO was formed, where the PL spectrum displays strong UV emission.^[22] Upon prolonging the heat treatment, the amorphous ZnO continuously turned into nanocrystalline ZnO, hence the quantum dot is gradually degenerated, so the *B* integrated intensity decreases along exponential decay, which can be understood in terms of quantum confinement, quantum size effects. The above discussion also indicates that the high-energy *L* band always appears simultaneously with amorphous ZnO, which reveals that the *L* band is associated with excitonic emission of amorphous ZnO. Interesting features are found in the *L* band energy. A question was raised why the peak energy of *L* band barely changes with increasing time. By carefully studying the heat decomposition process and complement with infrared spectra, we think that structure of amorphous ZnO is composed of amorphous ZnO cluster, which contains tens of ZnO molecules and keeps to be a certain stable structure. When the compound was fully turned into nanocrystalline ZnO, no *L* band can be detected. Study of dual excitonic emission should lead to a more complete description of the structure properties of amorphous

ZnO, which may be helpful to understand the dual excitonic emission.

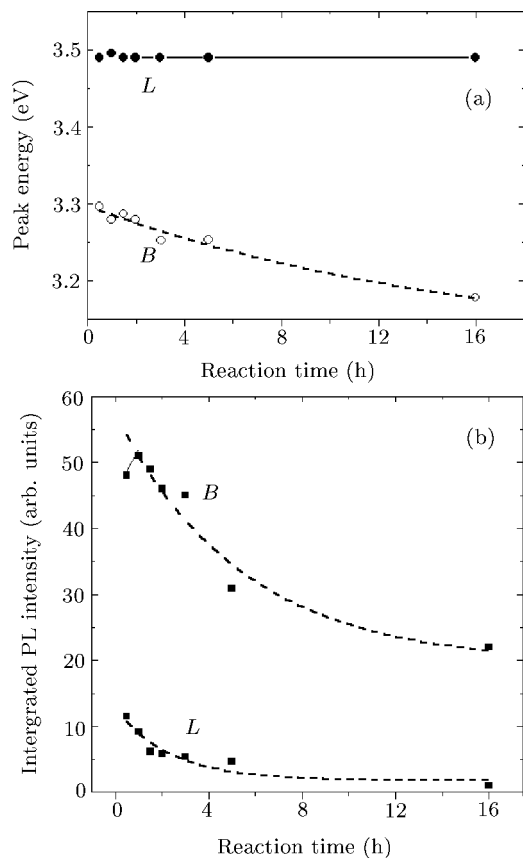


Fig. 5. (a) Heat treatment time dependence of the peak energy for *L* and *B* in the UV emission, respectively. (b) Heat treatment time dependence of the integrated PL intensity for *L* and *B*, respectively. The dashed lines are exponential fit.

In summary, dual excitonic emission has been investigated at room temperature. Our results indicate

that dual excitonic emission is originated from amorphous ZnO and nanocrystalline ZnO, respectively. The dual excitonic emission is always accompanying amorphous ZnO. The strong UV enhanced properties of amorphous ZnO are derived from quantum confinement effects.

References

- [1] Wu H Z, Xu X L, Qiu D J, He K M and Shou X 2000 *Chin. Phys. Lett.* **17** 694
- [2] Zou L, Ye Z Z, Huang J Y and Zhao B H 2002 *Chin. Phys. Lett.* **19** 1350
- [3] Noriko S, Haito H, Takashi S, Naoki O, Isao S and Kunihito K 2002 *Adv. Mater.* **14** 418
- [4] Huang M H et al 2001 *Science* **292** 1897
- [5] Deng Y, Chen Q, Yin Z and Chen W C 2002 *Chin. Phys. Lett.* **19** 372
- [6] Zhang X T et al 2002 *Chin. Phys. Lett.* **19** 127
- [7] Baganll D M, Chen Y F, Zhu Z and Yao T 1997 *Appl. Phys. Lett.* **70** 2230
- [8] Johnson C J, Yan H Q, Schaller R D and Haber L H 2001 *J. Phys. Chem. B* **105** 11387
- [9] Cao H, Xu J Y and Zhang D Z 2000 *Phys. Rev. Lett.* **84** 5584
- [10] Mitra A and Thareja R K 2001 *J. Appl. Phys.* **89** 2025
- [11] Spanhel L and Anderson M A 1991 *J. Am. Chem. Soc.* **113** 2826
- [12] Zhou H, Alves H, Hofmann D M, Kriegseis W and Meyer B K 2002 *Appl. Phys. Lett.* **80** 210
- [13] Wong E M and Searson P C 1999 *Appl. Phys. Lett.* **74** 2939
- [14] Dijken A V, Meulenkaamp E A, Vanmaekbergh D and Meijerink A 2000 *J. Phys. Chem. B* **104** 1715
- [15] Wang Z J et al 2003 *J. Mater. Res.* **18** 151
- [16] Wang Z J et al 2003 *Nanotechnol.* **13** 11
- [17] Fouquet J E and Siegman A E 1985 *Appl. Phys. Lett.* **46** 280
- [18] Klingshirn C 1975 *Phys. Status Solidi B* **71** 547
- [19] Reynolds D C and Collins T C 1969 *Phys. Rev.* **185** 1099
- [20] Louis B 1986 *IEEE J. Quantum Electron.* **22** 1909
- [21] Sun Y, Ketterson J B and Wong G K L 2000 *Appl. Phys. Lett.* **77** 2322
- [22] Klimov V I et al 2000 *Science* **290** 314